

Dynamics of electrons and phonons in semiconductors. II. Drag effects

N. Perrin and H. Budd*

Groupe de Physique des Solides, Ecole Normale Supérieure, 24 rue Lhomond, 75231 Paris 05, France

(Received 17 October 1973)

We present an analysis of the dynamics of the coupled electron-phonon system in the presence of an intense electric field in nondegenerate semiconductors. The effects of mutual electron-phonon drag are taken into account. The electron and phonon distribution functions are both assumed to be anisotropic, the isotropic part of the electron distribution being a Maxwell-Boltzmann distribution with a time-dependent electron temperature $T_e(t)$. Comparison is made with the results obtained in neglecting the anisotropy of the distribution functions. It is shown that the anisotropy of the electron and phonon distributions does not drastically change the qualitative evolution of the isotropic part of these distributions; the quantitative differences are functions of the carrier concentration. The stimulated emission of phonons is discussed.

I. INTRODUCTION

The application of an intense electric field to a semiconductor generally leads to significant deviations of the electron distribution function from its equilibrium value. The phonon distribution is also modified through the electron-phonon coupling,¹⁻⁴ and can also deviate considerably from its thermal equilibrium value when the phonon lifetime is long.⁴ This is the case for acoustic phonons at low temperatures.^{5,6}

Even for weak electric fields, where the electron drift velocity is small compared to the rms velocity, the phonons acquire a drift velocity parallel to that of the electrons. This phonon drag effect is well known since it manifests itself in an increased electron mobility. In an intense electric field, the electrons not only acquire a drift velocity but also acquire increased energy. The same is true of the phonon distribution.

Many theories^{1-4,7-9} of the steady-state electron mobility have been presented, taking account of phonon heating effects. Some of them have included a phonon drift term in their calculations.^{1,3,8} Sato concluded that this term is negligible for all phonon "temperatures." Conwell,⁸ on the other hand, showed that its effect on carrier transport can be considerable when the drift velocity of the carriers exceeds the sound velocity. Recently, some analyses of the time-dependent case have been undertaken.¹⁰⁻¹³ As in the steady-state situation, drastic simplifications have been made, due to the complexity of the coupled equations: Paranjape and Paranjape¹¹ gave an approximate analytic expression for the electric current, based on an isotropic phonon distribution function in which some time-dependent terms are approximated as constant. Yamashita and Nakamura,¹⁰ on the other hand, consider anisotropic distribution functions but neglect the carrier heating. In a previous paper,¹⁴ we presented a detailed theoretical study of the cou-

pled dynamics of carriers and phonons; the electron and phonon distribution functions were assumed to be isotropic. The coupled equations for the electron and phonon distributions were solved numerically for a model nondegenerate semiconductor, with a simple parabolic band structure, and an elastically isotropic crystal. In fact, for weak electric fields, the electrons are scattered quasi-elastically in the absence of optical modes, and the carrier distribution and therefore the phonon distribution are approximately isotropic.

However, the importance of the drift term in the phonon distribution has been shown experimentally¹⁵⁻¹⁷ at both strong and weak electric fields: Hubner and Shockley¹⁵ observed an effect of phonon drag on electrons in silicon; Ascarelli¹⁶ obtained evidence of the anisotropy of the phonon flux in germanium at high electric field (30 V cm⁻¹) and the stimulated emission of phonons by supersonic electrons was observed by Zylbersztein in *n*-Ge.¹⁷

In this paper, we report a theoretical study of the time dependence of the electron and phonon distribution functions, taking account of their anisotropic parts. We consider the interaction of phonons with the electrons and with the boundaries, but still neglect the phonon-phonon processes.¹⁴ We introduce a momentum boundary relaxation time τ_b^p , which is of the order of the phonon transit time L/c (L and c being an appropriate sample dimension and sound velocity, respectively), and an energy-boundary relaxation time τ_b^e which is different from the momentum relaxation time τ_b^p : $\tau_b^e = \eta L/c$, η being a numerical factor which measures the acoustic mismatch between the crystal and the heat bath.^{7,18} This is in the spirit of our previous work,¹⁴ and is the simplest fashion to include phonon interactions with the heat bath without becoming involved with spatially inhomogeneous distributions. As in our previous paper,¹⁴ the carrier concentration is assumed to be constant. Impurity scattering and intravalley acoustic-phonon scattering are the only

electron scattering processes considered. At low temperatures this is valid for moderate heating of the electron system. Strong heating of the electrons would require the inclusion of optical-mode scattering.¹⁹

A study of the time dependence of both the electron and phonon distribution functions requires the solution of the coupled electron-phonon transport equations which we set up in Sec. II, along with the numerical method used to obtain their numerical solution. As in Ref. 14 we consider a model non-degenerate semiconductor, with a simple band structure and an elastically isotropic crystal. In Sec. III, we present and discuss the results.

II. MODEL CALCULATION

A. Distribution functions for electrons and phonons

We write the carrier distribution $f(\vec{k})$ as the sum of two terms: a spherically symmetric term (or isotropic term) $f_0(\vec{k}) = f_0(\epsilon_k)$, which is taken to be a Maxwell-Boltzmann distribution characterized by a time-dependent electron temperature $T_e(t)$,^{14,20} and an asymmetric term (or drift term) $f_{an}(\vec{k})$,

$$f(\vec{k}) = f_0(\vec{k}) + f_{an}(\vec{k}) \quad , \quad (2.1)$$

$$f_0(\vec{k}) = f_0(\epsilon_k) = \frac{n}{N_c(T_e)} e^{-\epsilon_k/k_B T_e} \quad , \quad (2.2)$$

$$f_{an}(\vec{k}) = k_E f_1(\epsilon_k) \quad , \quad (2.3)$$

where k_E is the component of the carrier wave vector \vec{k} in the field direction. ϵ_k is the carrier energy,

$$\epsilon_k = \hbar^2 k^2 / 2m \quad ,$$

n , m , $N_c(T_e)$ being the carrier concentration, effective mass, and effective density of states, respectively, and

$$N_c(T_e) = 2(2\pi m k_B T_e / \hbar^2)^{3/2} \quad ,$$

where k_B is Boltzmann's constant.

Similarly, the phonon distribution $N(\vec{q})$ is assumed to be of the form

$$N(\vec{q}) = N_0(q) + q_E N_1(q) \quad , \quad (2.4)$$

where q_E is the component of the phonon wave vector \vec{q} along the electric field $q_E = q \cos(\vec{q}, \vec{E})$. N_0 is a spherically symmetric term and $q_E N_1$ is the asymmetric part of the phonon distribution function.

It must be emphasized that no assumption is made, either on the form of N_0 and N_1 , or on the form of f_1 in the electron distribution function. We have, however, restricted the anisotropies of the distributions by retaining only the first two Legendre polynomials in the general expansions of their angular dependence.

B. Coupled Boltzmann equations for electrons and phonons

The Boltzmann equation for the electrons gives

$$-\frac{e\vec{E}}{\hbar} \cdot \vec{\nabla}_k f + \hat{C}_a f + \hat{C}_I f = \frac{\partial f}{\partial t} \quad , \quad (2.5)$$

where e is the charge of the carriers ($e < 0$ for electrons), \vec{E} is the applied pulsed electric field, and \hat{C}_a and \hat{C}_I are the collision operators for acoustic phonon scattering and for impurity scattering, respectively. For the latter, we have

$$\hat{C}_I(f(\vec{k})) = \hat{C}_I(f_{an}(\vec{k})) = -k_E f_1(\epsilon_k) / \tau_I \quad , \quad (2.6)$$

where τ_I is the electron momentum relaxation time due to impurities. As usual, we take

$$\tau_I = C \epsilon_k^{3/2} \quad , \quad (2.7)$$

which leads to the following temperature dependence of μ_I :

$$\mu_I = \alpha T_e^{3/2} \quad , \quad (2.8)$$

α and C being constants determined from experimental results.^{14,21,22}

The phonon term is given by

$$\hat{C}_a f(\vec{k}) = D \sum_{\vec{q}} \omega_q \{ [f(\vec{k} + \vec{q}) N(\vec{q}) + 1] - f(\vec{k}) N(\vec{q}) \} \delta(\epsilon_{\vec{k} + \vec{q}} - \epsilon_k - \hbar \omega_q) + [f(\vec{k} - \vec{q}) N(\vec{q}) - f(\vec{k}) [N(\vec{q}) + 1]] \delta(\epsilon_k - \epsilon_{\vec{k} - \vec{q}} - \hbar \omega_q) \quad , \quad (2.9)$$

where D is a constant:

$$D = \frac{2\pi}{\hbar} \frac{E_1^2 \hbar}{2V \rho u^2} = \frac{\pi E_1^2}{V \rho u^2} \quad . \quad (2.10)$$

In Eq. (2.10), E_1 is the acoustic deformation-potential constant, ρ is the density of the crystal, and V is the volume of the crystal.²³

The anisotropic part of Eq. (2.9) only needs to be considered for the determination of $f_1(\epsilon_k)$. The nonlinear terms in q_E and k_E obtained in developing

the terms in the brackets of Eq. (2.9), using Eqs. (2.1)–(2.4), do not contribute to a drift of the carriers. They are irrelevant for the determination of $\hat{C}_a f_1$. Then we obtain

$$\hat{C}_a(f_1 k_E) = k_E [-f_1(\epsilon_k) / \tau_a - f_0(\epsilon_k) / x] \quad , \quad (2.11)$$

with

$$\frac{1}{\tau_a} = \frac{A}{k^3} \int_0^{2k} (N_0 + \frac{1}{2}) q^4 dq \quad (2.12)$$

and

$$\frac{1}{x} = -\frac{A}{k^3} \frac{\hbar\mu}{k_B T_e} \int_0^{2k} N_1 q^5 dq \quad (2.13)$$

A is a constant,

$$A = mE_1^2/4\pi\rho u\hbar^2 \quad .$$

τ_a is the usual momentum relaxation time for electrons on acoustic phonons and f_0/x arises from the anisotropy of the phonon distribution. This term is positive since the phonon drift is in the same direction as the electrons, i. e., $N_1 < 0$. Stated otherwise, the first term represents the momentum transfer from the drifting electrons to the isotropic phonons (N_0), while the second represents the momentum fed back to the electrons by the drifting phonons (N_1). In deriving these equations we have expanded the function $f_0(\epsilon_k \pm \hbar\omega)$ with respect to $\hbar\omega$, dropping terms involving powers of $\hbar\omega$ greater than the first:

$$f_0(\epsilon_k \pm \hbar\omega) = f_0(\epsilon_k) \pm \hbar\omega \frac{\partial f_0}{\partial \epsilon_k} \quad (2.14)$$

and

$$f_1(\epsilon_k \pm \hbar\omega) = f_1(\epsilon_k) \quad .$$

The expression for $f_1(\epsilon_k)$ is obtained from Eqs. (2.5), (2.7), and (2.11): we assume a quasistationary value of the electron distribution $f(\vec{k})$ ($\partial f/\partial t = 0$) corresponding to the instantaneous values of the phonon distribution and electron temperature. This is justified by the extremely short electron-momentum relaxation time.¹⁴ Then

$$f_1(\epsilon_k) = -\frac{f_0 |e| \hbar}{mk_B T_e} \tau(1+G)E \quad , \quad (2.15)$$

with

$$\tau^{-1} = \tau_a^{-1} + \tau_I^{-1} \quad (2.16)$$

and

$$G = \frac{mk_B T_e}{|e| E \hbar} \frac{1}{x} \quad . \quad (2.17)$$

We see that $f_1(\epsilon_k)$ is a function of T_e and $N(\vec{q})$. The current density may be written in the usual form

$$j = n |e| \mu E \quad ,$$

where μ is given by

$$\mu = (|e|/m) \langle \tau' \rangle \quad , \quad (2.18)$$

with

$$\tau' = (1+G)\tau \quad .$$

The G term, arising from the anisotropy of the phonon distribution, increases the relaxation time, and therefore, the carrier mobility.

The rate of change of the phonon distribution due to the electrons is given by

$$\left(\frac{\partial N}{\partial t}\right)_e = D \sum_{\vec{k}} \omega_q \{ [N(\vec{q}) + 1] f(\vec{k}) \delta(\epsilon_{\vec{k}-\vec{q}} + \hbar\omega_q - \epsilon_k) - N(\vec{q}) f(\vec{k}) \delta(\epsilon_{\vec{k}+\vec{q}} - \hbar\omega_q - \epsilon_k) \} \quad . \quad (2.19)$$

It is straightforward to see that nonlinear terms in q_E and k_E are obtained in developing Eq. (2.19), with the use of Eqs. (2.1), (2.4), and (2.14).

These terms may be neglected only if the asymmetric parts of the phonon and electron distribution functions are small. They are included in the following equations where, for consistency, we only retain the first two Legendre polynomials in $\cos(\vec{q}, \vec{E})$:

$$\left(\frac{\partial N_0}{\partial t}\right)_e = \frac{\bar{N}(T_e) - N_0}{\tau_{\text{eff}}} + BN_1 \quad , \quad (2.20)$$

with

$$\frac{1}{\tau_{\text{eff}}(q, T_e)} = \frac{n\pi^{1/2} m^{1/2} E_1^2}{2^{1/2} \hbar \rho u (k_B T_e)^{1/2} \bar{N}(T_e)} \times \exp\left[-\frac{\hbar^2}{2mk_B T_e} \left(\frac{q}{2} + \frac{mu}{\hbar}\right)^2\right] \quad , \quad (2.21)$$

where $\bar{N}(T_e)$ is the Planck distribution at temperature T_e .²⁴

$$D_1 = DV/8\pi^3$$

and

$$B = \frac{4\pi}{3} D_1 \frac{m^3}{\hbar^6} \left[\left(\hbar\omega_q + \frac{\hbar^2 q^2}{2m} \right) \int_{\epsilon(q/2+mu/\hbar)}^{\infty} f_1(\epsilon_k) d\epsilon_k - \left(\hbar\omega_q - \frac{\hbar^2 q^2}{2m} \right) \int_{\epsilon(q/2-mu/\hbar)}^{\infty} f_1(\epsilon_k) d\epsilon_k \right] \quad . \quad (2.22)$$

For most of the phonons, at least for $q > 2mu/\hbar$, B is negative and the BN_1 term enhances the heating of the phonons since $N_1 < 0$, $BN_1 > 0$. This arises from the mutual drag of phonons and electrons. B is equal to zero when the nonlinear terms in k_E and q_E are neglected.

Equation (2.19) yields for the anisotropic part of the phonon distribution

$$\left(\frac{\partial N_1}{\partial t}\right)_e = -\frac{N_1}{\tau_{\text{eff}}} + \left(\frac{N_0}{R_1} + \frac{1}{R_2}\right) \frac{4\pi D_1 u m^2}{\hbar^4} \quad , \quad (2.23)$$

with

$$\frac{1}{R_2} = \left(\frac{1}{2} + \frac{mu}{\hbar q} \right) \int_{\epsilon(q/2+mu/\hbar)}^{\infty} f_1(\epsilon_k) d\epsilon_k, \quad (2.24)$$

$$\frac{1}{R_1} = \frac{1}{R_2} + \left(\frac{1}{2} - \frac{mu}{\hbar q} \right) \int_{\epsilon(q/2-mu/\hbar)}^{\infty} f_1(\epsilon_k) d\epsilon_k; \quad (2.25)$$

the two terms $1/R_2$ and N_0/R_1 express the electron drag on the phonons.

The total rate of change of the phonon distribution is

$$\frac{\partial N}{\partial t} = \left(\frac{\partial N}{\partial t} \right)_e + \left(\frac{\partial N}{\partial t} \right)_b, \quad (2.26)$$

where the rate of change due to the heat bath $(\partial N/\partial t)_b$ is given by

$$\left(\frac{\partial N_0}{\partial t} \right)_b = \frac{\bar{N}(T_0) - N_0}{\tau_b^\epsilon} \quad (2.27)$$

and

$$\left(\frac{\partial N_1}{\partial t} \right)_b = -\frac{N_1}{\tau_b^p}, \quad (2.28)$$

where τ_b^ϵ and τ_b^p are the relaxation times discussed in Sec. I, and T_0 is the heat-bath temperature.

The evolution of both the electron and phonon distributions can be determined from Eqs. (2.5)–(2.28), and from the usual energy-balance equation for electrons:

$$\left\langle \frac{d\epsilon}{dt} \right\rangle = \mu e E^2 - \frac{1}{nV} \sum_{\vec{q}} \hbar \omega_{\vec{q}} \left(\frac{\partial N(\vec{q})}{\partial t} \right)_e. \quad (2.29)$$

The $\langle d\epsilon/dt \rangle$ term will be neglected, according to our adiabatic approximation,¹⁴ which leads to the following energy-balance equation:

$$\mu e E^2 = \frac{1}{nV} \sum_{\vec{q}} \hbar \omega_{\vec{q}} \left(\frac{\partial N(\vec{q})}{\partial t} \right)_e. \quad (2.30)$$

C. Numerical method

We have solved the evolution equations on an IBM 370.165 for a typical *n*-type nondegenerate semiconductor. The numerical method is similar to that in our previous paper.¹⁴ Initial values of $f_1^0 \neq 0$, $T_e^0 \neq T_0$ of the electron distribution are determined immediately after the application of the electric field to the equilibrium system at temperature $T_0 = 4.2^\circ\text{K}$. The phonon distribution remains at equilibrium in this initial step [$N_0 = \bar{N}(T_0)$, $N_1 = 0$]. Then the variations δN_0 and δN_1 of the phonon distribution during a small time interval Δt are calculated from Eqs. (2.20)–(2.28). The variation δT_e of the electron temperature, which is necessary to maintain the energy balance [Eq. (2.30)], is then calculated. The value of f_1 corresponding to these modified values of $N(\vec{q})$ and $T_e(t)$ is calculated from Eq. (2.15). We then proceed to the next step, at $t = 2\Delta t$ and so on. The time interval Δt is chosen so that

$$\Delta t / (\tau_\alpha)_{\min} \ll 1,$$

τ_α being either τ_{ep} , τ_b^p , or τ_b^ϵ .¹⁴

Numerical calculations have been performed for different carrier concentrations. The effective electron mass is taken as $m = 0.25m_0$, m_0 being the free-electron mass, and the acoustic deformation-potential constant is assumed to be $E_1 = 10 \text{ eV}$.¹⁴ The mean sound velocity is taken as $u = 5.4 \times 10^5 \text{ cm sec}^{-1}$. We assume $\tau_b^\epsilon = 25\tau_b^p$ with $\tau_b^p = 0.2 \mu\text{sec}$.

III. RESULTS

In Figs. 1–11 are shown some of the results obtained in neglecting the nonlinear terms in q_E and k_E [$B = 0$ in Eq. (2.20)]. This approximation will be discussed later. We have verified that it is quite valid here and leads to errors of a few percent. We also compare with results obtained in neglecting the anisotropic terms in the distribution functions (referred to as the I case).

A. Electron temperature and mobility

In Fig. 1 we present the time dependence of the electron temperature T_e , for different carrier concentrations and electric fields. According to our adiabatic approximation,¹⁴ the initial temperature T_e^0 reached by the electrons immediately after the application of the electric field, depends only on the

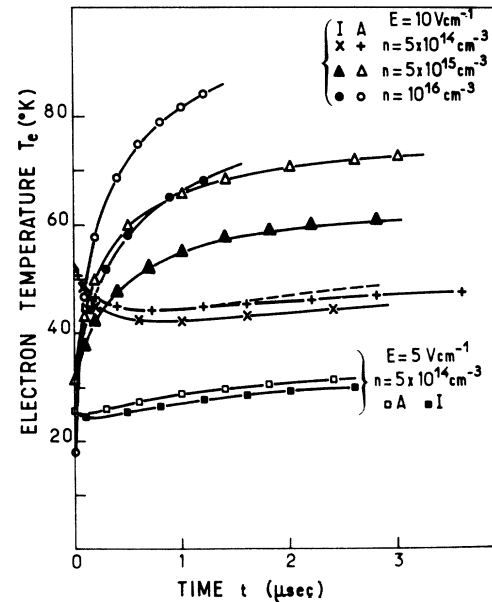


FIG. 1. Electron temperature $T_e(t)$ vs time t for different carrier concentrations n . The anisotropic terms of the distribution functions, included in the A case, have been neglected in the I case for comparison. The dashed line represents the electron temperature obtained for a different value of the acoustic mismatch parameter $\eta = \tau_b^\epsilon / \tau_b^p = 100$ with $\tau_b^p = 0.2 \mu\text{sec}$ ($n = 5 \times 10^{14} \text{ cm}^{-3}$, $E = 10 \text{ V cm}^{-1}$).

thermal-equilibrium phonon distribution and is therefore the same value in this case (referred to as the A case), where the anisotropy of the distribution functions is considered, and in the I case. The two types of behavior exhibited by the electron temperature in the I case¹⁴ are still present in the A case. The electron temperature in the latter case T_e^A is seen to be larger than the electron temperature T_e^I in the I case, the difference $T_e^A - T_e^I$ increasing with carrier concentration n and with time. This is due to the phonon drag effect as discussed below, which becomes larger for high n .

The time dependence of the mobility μ is shown in Fig. 2 and a comparison is made with the mobility in the I case. As in the latter case, the mobility is seen to decrease with time except in the lowest curve. The variation of the mobility in the A case is still more complicated than in the I case, since in addition to its nonmonotonic dependence on T_e and its decrease with N_0 ,¹⁴ there is its N_1 dependence. We see in Fig. 2, by comparison with the I case, that the latter increases the mobility as expected from Eqs. (2.13), (2.17), and (2.18). This increase of the mobility is due to a phonon drag on the electrons, which is most significant for large carrier concentrations. If we consider the energy balance equation [Eq. (2.30)] along with Eqs. (2.18) and (2.20) ($B=0$ here), the increase in mobility (and therefore the phonon drag on the electrons) explains the difference $T_e^A - T_e^I$ of the electron temperatures observed in Fig. 1, and its variation with carrier concentration.

B. Phonon distribution: Isotropic part

The monotonic increase with time of N_0 , the iso-

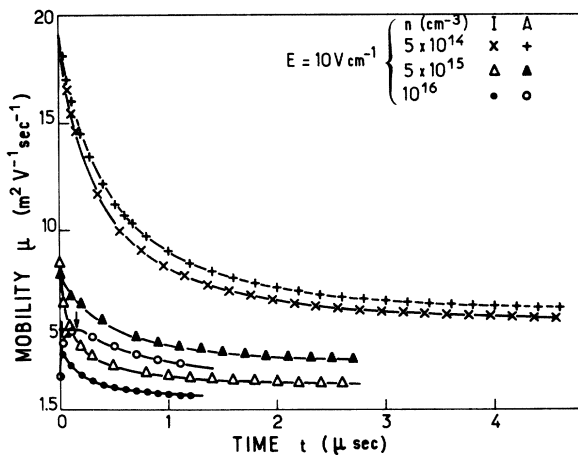


FIG. 2. Electron mobility μ vs time t for different carrier concentrations. In the I case, the anisotropy of the distributions have been neglected for comparison with the A case.

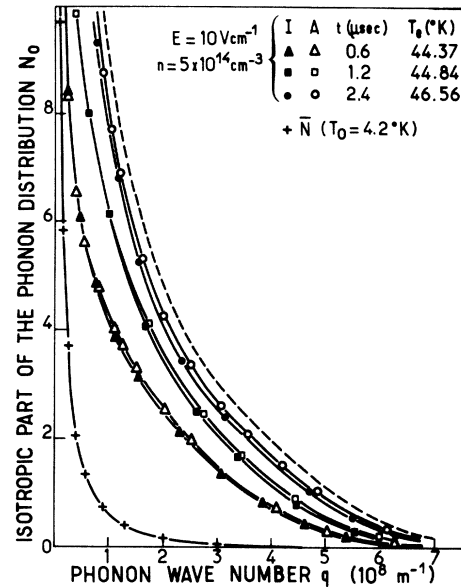


FIG. 3. Isotropic part of the phonon distribution N_0 vs phonon wave number q at different times (A case) for a carrier concentration $n = 5 \times 10^{14} \text{ cm}^{-3}$. The curves in the I case are shown for comparison: They represent the phonon distribution N_q^I obtained in neglecting the anisotropy of the distribution functions. The upper curve corresponds to the steady state. The dashed line represents the isotropic part of the phonon distribution obtained for a different value of the acoustic mismatch parameter $\eta = 100 = \tau_b^I / \tau_b^A$ ($\tau_b^I = 0.2 \text{ } \mu\text{sec}$) at time $2.4 \text{ } \mu\text{sec}$.

tropic part of the phonon distribution, is seen in Figs. 3 and 4 for two carrier concentrations. It is compared with the phonon distribution N_q^I in the I case. We see that N_0 is only slightly larger than N_q^I , the difference $N_0 - N_q^I$ increasing with time and with carrier concentration. This difference is essentially determined by the difference of the electron temperatures at the same times as can be seen from Fig. 4, where we compare N_0 to N_q^I corresponding to approximately the same temperature ($T_e \approx 64.2^\circ \text{K}$) and of course, to a different time. It is seen that N_q^I ($T_e = 64.27^\circ \text{K}$) only deviates appreciably from N_0 for high-energy phonons. This is characteristic of the phonon distributions obtained in the I case for two values of the electric field (at given concentration and temperature), as is shown in the inset of Fig. 4, where N_q^I ($E = 5 \text{ V cm}^{-1}$) deviates from N_q^I ($E = 10 \text{ V cm}^{-1}$) in the same way. Therefore, the isotropic part of the phonon distribution N_0 behaves exactly as N_q^I would do for a higher electric field (at given concentration and temperature). This is due to a phonon drag on the electrons as can be expected from Eq. (2.15), where the $(1+G)E$ term (function of the qN_1 term of the phonon distribution) could be interpreted as an effective electric field, larger than E ($G > 0$).

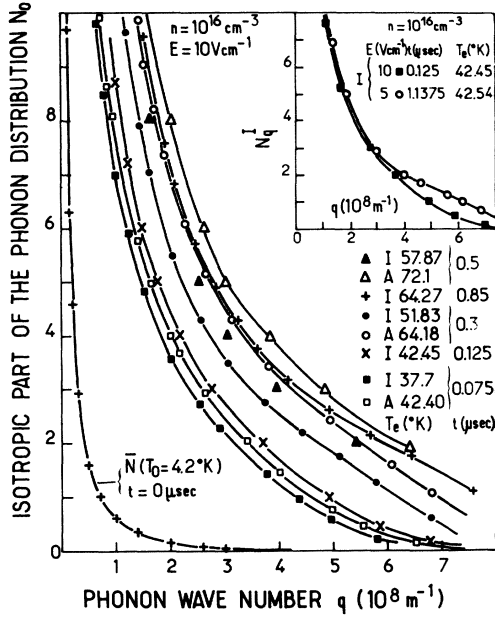


FIG. 4. Isotropic part of the phonon distribution N_0 vs phonon wave number q at different times for a carrier concentration $n = 10^{16} \text{ cm}^{-3}$. The curves in the I case are shown for comparison. The curves in the inset represent the phonon distribution N_0^I obtained in the I case at about the same temperature, for two values of the electric field.

C. Electron differential mobility

The evolution of the differential drift velocity $v(\epsilon_k)$ defined by writing Eq. (2.15) in the form

$$f_1(\epsilon_k) = -\hbar v_1(\epsilon_k) \frac{\partial f_0}{\partial \epsilon_k} = -\frac{\hbar}{k_B T_e} v(\epsilon_k) f_0 \quad (3.1)$$

is shown in Fig. 5 for a carrier concentration $n = 5 \times 10^{14} \text{ cm}^{-3}$ and an electric field $E = 10 \text{ V cm}^{-1}$.

Equations (2.15) and (3.1) give

$$v_1(\epsilon_k) = -(|e|/m) \tau(1+G)E = -v(\epsilon_k) \quad (3.2)$$

In Fig. 6 is shown the time dependence of the differential mobility $\mu(\epsilon_k) = v(\epsilon_k)/E$, for an electric field and a carrier concentration different from that of Fig. 5:

$$\mu(\epsilon_k) = |e|(\tau/m)(1+G) \quad (3.3)$$

It is seen that the mobility $\mu(\epsilon_k)$ [or the velocity $v(\epsilon_k)$] decreases with time. We note that the curves have a maximum for an energy ϵ_M , whose position is a function of the carrier concentration and of the electric field: ϵ_M may be a monotonically decreasing function of time as in Fig. 5, or it may first increase and then decrease with time as in Fig. 6. The maximum at time $t=0$ ($N_1=0$, $1/X=0 \rightarrow G=0$) simply reflects the maximum of the electron relaxation time $\tau(\epsilon_k)$; as expected from Eqs. (2.7),

(2.12), and (2.16) $\tau(\epsilon_k)$ has a maximum, $\tau_I(\epsilon_k)$ being an increasing function of ϵ_k [Eq. (2.7)], and $\tau_a(\epsilon_k)$ being a decreasing function of ϵ_k . Therefore, the increasing part of the curve $v(\epsilon_k)$ [or $\mu(\epsilon_k)$] corresponds to dominant impurity scattering, and the decreasing part of the curve $v(\epsilon_k)$ [or $\mu(\epsilon_k)$] corresponds to dominant phonon scattering. The slope of the curve, for small energy ϵ_k , depends essentially on the constant C in Eq. (2.7), which is a decreasing function of the carrier concentration.

Therefore, ϵ_M^0 at time $t=0$ is expected to be larger for larger carrier concentrations (the phonon distribution at this time is the thermal equilibrium distribution of 4.2 °K). Indeed, we observe in Figs. 5 and 6 that ϵ_M^0 ($n = 5 \times 10^{15} \text{ cm}^{-3}$) $>$ ϵ_M^0 ($n = 10^{14} \text{ cm}^{-3}$). Let us consider the evolution of ϵ_M with time. If the term N_1 remained rigorously equal to zero, the maximum of $\mu(\epsilon_k)$ would move towards smaller ϵ_M as expected from the increasing number of randomly directed phonons N_0 (τ being a decreasing function of N_0). The presence of the anisotropic term N_1 can provoke a displacement of the maximum of $\mu(\epsilon_k)$ either to higher or lower energies. The maximum is determined by the condition

$$\frac{dG/d\epsilon_k}{G+1} = -\frac{d\tau/d\epsilon_k}{\tau} \quad (3.4)$$

We now see from Eqs. (2.13) and (2.17) that G is zero, both for small or large k , so that $dG/d\epsilon_k$ can be positive or negative. Therefore, from Eq. (3.4) the maximum may be displaced in either direction. To see this explicitly in a simple case, we consider a small phonon drift term N_1 such that $1+G=1$:

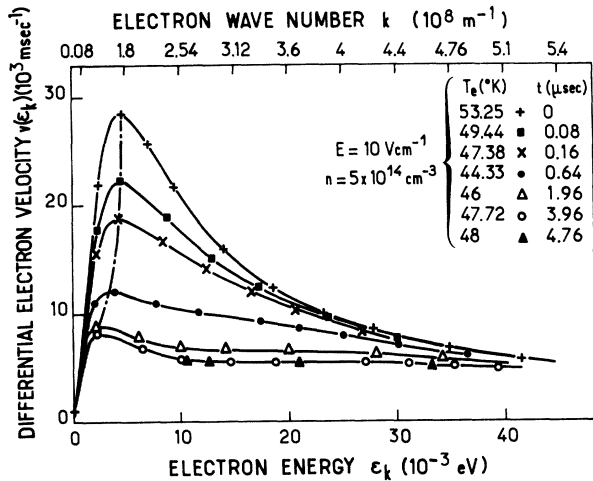


FIG. 5. Differential drift velocity $v(\epsilon_k)$ vs electron energy ϵ_k at different times for a carrier concentration $n = 5 \times 10^{14} \text{ cm}^{-3}$. The lower curve corresponds approximately to the steady state.

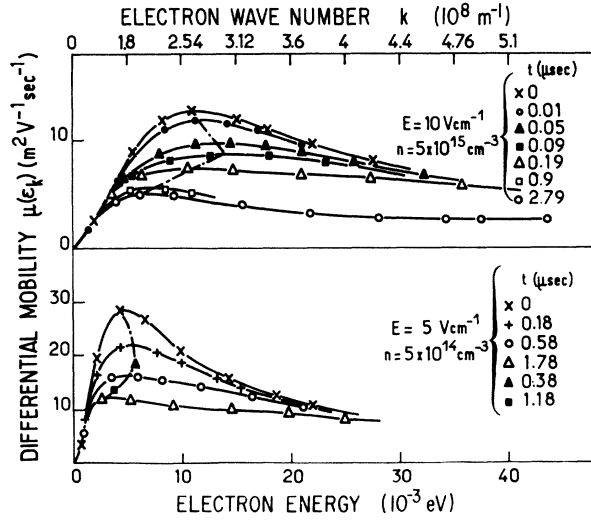


FIG. 6. Differential electron mobility $\mu(\epsilon_k)$ vs electron energy for different carrier concentrations and electric fields, at different times. The dashed-dotted lines represent the approximate position of the maxima.

$$\frac{dG}{d\epsilon_k} \approx -\frac{d\tau/d\epsilon_k}{\tau};$$

$dG/d\epsilon_k = 0$ corresponds to the value of ϵ_M^0 for $N_1 = 0$ and the sign of $(dG/d\epsilon_k)_{\epsilon_M}$ will determine the sense of the displacement of ϵ_M for $N_1 \neq 0$. The form of $-(d\tau/d\epsilon_k)/\tau$ is shown in Fig. 7; in the vicinity of the cross point ϵ_M^0 , we see that ϵ_M increases for $G' = dG/d\epsilon_k > 0$ and decreases for $G' < 0$. Therefore, the nonmonotonic variation of ϵ_M with time is due to the anisotropy of the phonon distribution: the loss of electron momentum in the scattering by the phonons is smaller, since the phonons are drifted in the same direction as that of the electrons. This is one aspect of the phonon drag effect on the electrons.

The time dependence of the differential drift mobility is essentially determined by the increase of N_0 with time. This obviously leads to a reduction of τ , particularly in the intermediate range of energy. At low energies, τ is independent of N_0 since impurity scattering is dominant in this energy range. τ is also independent of N_0 at very large energies, where it tends to the zero-point limit. This, along with the q dependence of the phonon heating¹⁴ in the intermediate range of energy, leads to a general flattening of the $\mu(\epsilon_k)$ [or $v(\epsilon_k)$] vs ϵ_k curve.

D. Phonon distribution: Anisotropic part

A typical evolution of the anisotropic part of the phonon distribution function is shown in Figs. 8 and 9. The function $|qN_1|$ of q is seen to have a maximum whose position varies with time. At very

small time ($t \approx 0$), immediately after the application of the electric field to the equilibrium system, $|qN_1|$ arises from an electron drag on the phonons, the electrons transferring momentum to the phonons. It therefore only depends on the amplitude and form of $v(\epsilon_k)$. The evolution of $|qN_1|$ is complicated, since it depends on N_0 as well as on the differential velocity of the carriers, and on the relaxation times τ_{ep} and τ_b^p . The dependence on τ_b^p is negligible for sufficiently small times ($t \ll \tau_b^p$). The relative importance of N_0 and $v(\epsilon_k)$ determines the form of $|qN_1|$ and particularly the position of the maximum. A relatively small carrier concentration ($n = 5 \times 10^{14} \text{ cm}^{-3}$) tends to make the maximum of $|qN_1|$ only weakly N_0 dependent (Fig. 8), while a large concentration [which reduces $v(\epsilon_k)$ and its variation with ϵ_k , and produces a large heating of the phonons, even for small times] tends to make $|qN_1|$ strongly N_0 dependent (Fig. 9). The rate of increase of $|qN_1|$ decreases with time, which is expected since the momentum exchange between the carriers and the phonon decreases as $|qN_1|$ increases.

The ratio $|qN_1|/N_0$, characterizing the anisotropy of the phonon distribution, is seen in Fig. 10 for a carrier concentration $n = 10^{16} \text{ cm}^{-3}$. It is seen to be a nonmonotonic function of q at a given time, and a nonmonotonic function of time for a given wave number q . The evolution of $|qN_1|/N_0$ is essentially determined by the carrier differential velocity $v(\epsilon_k)$ and by the relaxation time τ_{ep} . The variation of $1/\tau_{ep}$ with q is shown in Fig. 11 for different temperatures. The relaxation time τ_{ep}

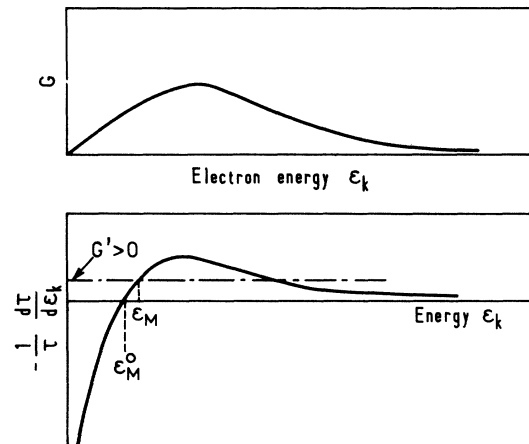


FIG. 7. Upper curve represents the form of the ϵ_k dependence of the G term which is a function of the anisotropy of the phonon distribution. G is related to the differential mobility by $\mu(\epsilon_k) = (1 + G) |e| \tau / m$. The lower curve represents the variation of the logarithmic derivative of the electron relaxation time τ with the energy ϵ_k .

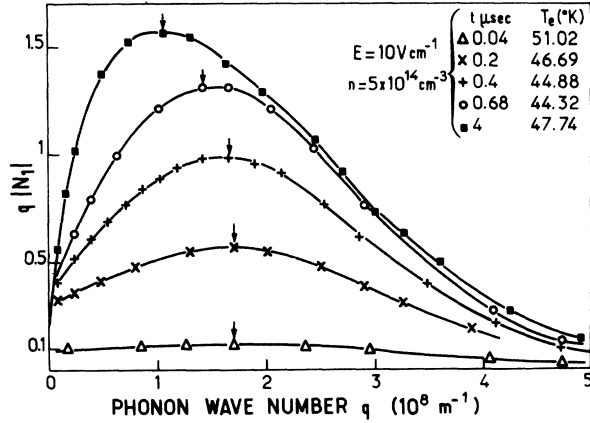


FIG. 8. Anisotropic part of the phonon distribution vs phonon wave number q at different times for a carrier concentration $n = 5 \times 10^{14} \text{ cm}^{-3}$.

may be sufficiently large for the high-frequency phonons to explain the kink observed in the curve of Fig. 10 for $t = 0.075 \mu\text{sec}$ [here $T_e = 42.85 \text{ }^\circ\text{K}$ and $1/\tau_{\infty} (q = 6 \times 10^8 \text{ m}^{-1}) \sim 0$], and the displacement of the maximum for $t = 0.025 \mu\text{sec}$. With increasing time, the ratio $|qN_1|/N_0$ decreases since momentum relaxation due to the boundaries becomes important, and in addition the electron drift velocity decreases.

E. Stimulated emission of phonons

The phenomenon of stimulated phonon emission is not obvious in our formulation of the coupled dynamics of electrons and phonons, since a direct

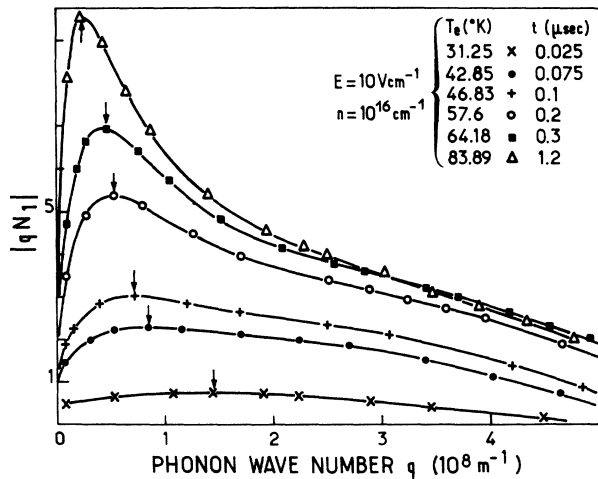


FIG. 9. Anisotropic part of the phonon distribution vs phonon wave number q at different times, for a carrier concentration $n = 10^{16} \text{ cm}^{-3}$.

comparison of the sound velocity to the mean drift velocity, $v_D = \mu E$, of the carriers is not possible in the expression of the total phonon rate of change.^{8,10} However, this latter $\partial N(\vec{q})/\partial t$ may be written in the form

$$\frac{\partial N(\vec{q})}{\partial t} = \xi + \beta N(\vec{q}), \quad (3.5)$$

where ξ is independent of N and β is generally an attenuation coefficient ($\beta < 0$). In fact, $\beta > 0$ corresponds to stimulated emission of phonons of wave vector \vec{q} .

Though the mean drift velocity v_D of the carriers is always larger than the sound velocity ($u = 5.4 \times 10^5 \text{ cm sec}^{-1}$) for the case $n = 5 \times 10^{14} \text{ cm}^{-3}$, $E = 10 \text{ V cm}^{-1}$, as can be seen in the upper curve of Fig. 2, the stimulated emission of phonons is only observed in our calculations [$\beta > 0$ in Eq. (3.5)] until time $t \approx 0.10 \mu\text{sec}$ (the mean carrier drift velocity being then $v_D = 16 \times 10^5 \text{ cm}^{-1}$). This arises from the phonon relaxation times which increase the threshold velocity for the onset of stimulated emission; then, the drift velocity v_D must be compared to an effective sound velocity u^* ,¹⁰ larger than the real sound velocity u . In the case just considered ($n = 5 \times 10^{14} \text{ cm}^{-3}$, $E = 10 \text{ V cm}^{-1}$, $\tau_b^e = 0.2 \mu\text{sec}$) the short boundary relaxation time τ_b^p of the phonons is expected to give a large effective sound velocity. In fact, with relaxation times $\tau_b^e = 1 \mu\text{sec}$ and $\tau_b^p = 100 \mu\text{sec}$, the stimulated emission still exists at time $t \approx 0.6 \mu\text{sec}$ ($v_D = 11 \times 10^5 \text{ cm sec}^{-1}$). However, in both cases, it is no longer visible in the steady state.

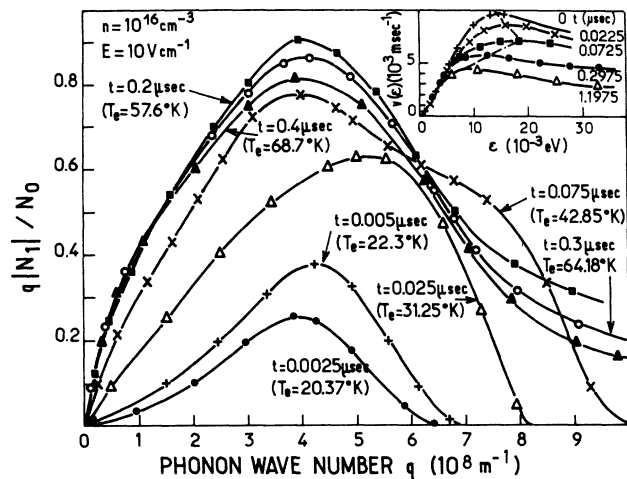


FIG. 10. Ratio of the anisotropic to isotropic part of the phonon distribution vs wave number q at different times for a carrier concentration $n = 10^{16} \text{ cm}^{-3}$. The corresponding electron differential velocity vs energy is shown in the inset.

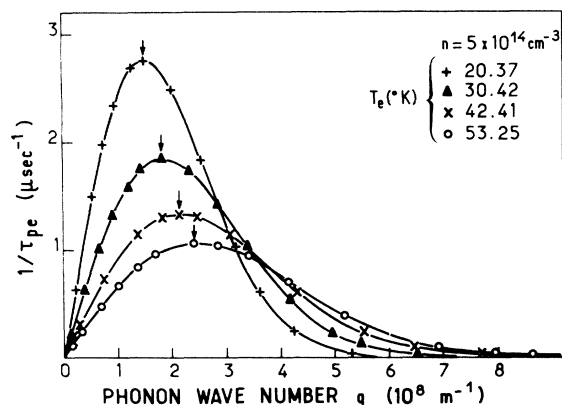


FIG. 11. Electron-phonon relaxation frequency $1/\tau_{ep}$ vs phonon wave number q for different electron temperatures.

The most serious deficiency of our treatment lies in neglecting all but the two lowest-order Legendre polynomials in the expansion of the distribution functions. For phonons traveling parallel to the sample surfaces, the effective τ_b^e and τ_b^p are infinite and under stimulated-emission conditions the distribution functions must become extremely anisotropic. A consistent treatment of the electron-phonon system taking into account these difficulties poses severe computational problems which are beyond the scope of this paper.

F. Nonlinear terms

So far we have neglected the nonlinear terms in q_E and k_E . The results obtained without neglecting these terms are only slightly different from those presented above. For instance, with $n = 5 \times 10^{14} \text{ cm}^{-3}$, $E = 10 \text{ V cm}^{-1}$, the electron temperature curve lies between the curves of the A and I cases in Fig. 1, and the variation of the phonon distribution is about a few percent, giving a slightly larger phonon distribution (Fig. 3), as discussed in Sec. II 3. The nonlinear terms enhance the stimulated emission of phonons. However, all these effects are small and therefore the nonlinear terms in q_E and k_E may be neglected.

G. Acoustic mismatch parameter

In all our calculations, we have taken the acoustic mismatch parameter $\eta = 25$. A different value of η ($\eta = 100$) has also been introduced for comparison (for $n = 5 \times 10^{14} \text{ cm}^{-3}$, $E = 10 \text{ V cm}^{-1}$). The re-

sults are presented in Figs. 1 and 3 with $\tau_b^e = 0.2 \text{ μsec}$ and $\tau_b^p = 20 \text{ μsec}$. It is seen that the variations of $T_e(t)$ and $N(\vec{q})$ are small, the most significant deviations appearing at times $t \geq \tau_b^e = 5 \text{ μsec}$ (the energy relaxation time first considered), which is a fairly large time for the electric pulses generally employed in semiconductors. Therefore, the considered variations of τ_b^e (which has been chosen in our calculation smaller than the value for Ge deduced from the reflection and transmission of elastic waves⁷) and η do not drastically change the results.

CONCLUSION

The results presented above show that the essential qualitative features of the response of a semiconductor to an intense electric field at low temperature are not drastically dependent on the effective anisotropy of both the electron and phonon distribution functions. Large deviations of the phonon and electron distributions from the equilibrium values are observed. The same qualitative time dependence of the electron temperature is found.¹⁴ We have, however, shown the importance of electron-phonon drag effects which significantly modify the quantitative results obtained for the electrons in neglecting the anisotropy of the distribution functions.

Stimulated emission of phonons is seen to be possible for intermediate carrier concentrations and short times. These latter results would be enhanced by a larger boundary momentum phonon relaxation time. In fact, the effective relaxation times τ_b^e and τ_b^p for phonons traveling parallel to the sample surfaces are infinite, and in the stimulated-emission conditions the phonon distribution becomes strongly anisotropic. This regime is poorly treated in this paper, where only the two lowest-order Legendre polynomials in the expansion of the distribution functions are considered. However, the heating of the phonons enhances the phonon-phonon interaction; hence the phonon relaxation time could become smaller than the boundary relaxation time, particularly for short-wavelength phonons.^{25,26} Therefore, a large increase of the boundary relaxation time without the introduction of the phonon-phonon scattering mechanism would not be realistic.

The energy dependence of the carrier differential velocity $v(\epsilon_k)$ shows that the assumption of an energy independent drift velocity would have been a crude approximation.

*Present address: Centre National de la Recherche Scientifique, 972 Fifth Avenue, New York, N.Y. 10021.
¹J. E. Parrott, Proc. Phys. Soc. Lond., **70**, 590 (1957).
²V. V. Paranjape, Proc. Phys. Soc. Lond., **80**, 971 (1962).

³H. Sato, J. Phys. Soc. Jap. **18**, 55 (1963).

⁴E. M. Conwell, Phys. Rev. **135**, A 814 (1964).

⁵C. Herring, Phys. Rev. **96**, 1163 (1954).

⁶T. H. Geballe and G. W. Hull, Phys. Rev. **94**, 1134 (1954).

- ⁷L. E. Gurewitsch and T. M. Gasymov, Fiz. Tverd. Tela 9, 106 (1967)[Sov. Phys. -Solid State 9, 78 (1967)].
- ⁸E. M. Conwell, Phys. Lett. 13, 285 (1964).
- ⁹A. Zylbersztejn and E. M. Conwell, Phys. Rev. Lett. 11, 417 (1963).
- ¹⁰J. Yamashita and K. Nakamura, Prog. Theor. Phys. 33, 1022 (1965).
- ¹¹V. V. Paranjape and B. V. Paranjape, Phys. Rev. 166, 757 (1968).
- ¹²K. Baumann, P. Kocevar, and M. Kriechbaum, J. Phys. Chem. Solids, 31, 95 (1970).
- ¹³K. Baumann, M. Kriechbaum, and H. Kahlert, J. Phys. Chem. Solids, 31, 1163 (1970).
- ¹⁴N. Perrin and H. Budd, Phys. Rev. B 6, 1359 (1972).
- ¹⁵K. Hubner and W. Shockley, Phys. Rev. Lett. 4, 504 (1960).
- ¹⁶G. Ascarelli, Phys. Rev. Lett. 5, 367 (1960).
- ¹⁷A. Zylbersztejn, Phys. Rev. Lett. 19, 838 (1967).
- ¹⁸L. D. Landau and E. M. Lifshitz, *Mechanics of Continuous Media* (Addison-Wesley, New York, 1958).
- ¹⁹P. Kocevar, J. Phys. C 5, 3349 (1972).
- ²⁰H. Frohlich and B. V. Paranjape, Proc. Phys. Soc. B 69, 29 (1956).
- ²¹P. P. Debye and E. M. Conwell, Phys. Rev. 93, 693 (1953).
- ²²F. J. Blatt, Phys. Rev. 105, 1203 (1957).
- ²³E. M. Conwell, in *Solid State Physics*, edited by F. Seitz and D. Turnbull (Academic, New York, 1957) Suppl. 9, pp. 108 and 219.
- ²⁴J. M. Ziman, Philos. Mag. 1, 191 (1956).
- ²⁵C. Herring, Phys. Rev. 96, 1163 (1954).
- ²⁶E. M. Conwell, in Ref. 23, p. 244.